

# Practical Methods to Estimate Fabric Mechanics from Metadata

H. Dominguez-Elvira<sup>1,2</sup>  and A. Nicas<sup>1</sup>  and G. Cirio<sup>1</sup>  and A. Rodríguez<sup>1</sup>  and E. Garces<sup>1,2</sup> 

<sup>1</sup>SEDDI, Madrid, Spain

<sup>2</sup>Universidad Rey Juan Carlos, Madrid, Spain



**Figure 1:** (updated figure) Using only fabric metadata as input (family, thickness, composition, density), or a flat image of the fabric if family information is not available, our methods estimate the mechanical parameters of fabrics in a few seconds without the need of special digitization equipment (left). Fabrics estimated this way show similar drapes to their ground truth counterpart, digitized using special testing devices producing stretch and bending data in a process that can take hours (right).

## Abstract

Estimating fabric mechanical properties is crucial to create realistic digital twins. Existing methods typically require testing physical fabric samples with expensive devices or cumbersome capture setups. In this work, we propose a method to estimate fabric mechanics just from known manufacturer metadata such as the fabric family, the density, the composition, and the thickness. Further, to alleviate the need to know the fabric family –which might be ambiguous or unknown for nonspecialists– we propose an end-to-end neural method that works with planar images of the textile as input. We evaluate our methods using extensive tests that include the industry standard Cusick and demonstrate that both of them produce drapes that strongly correlate with the ground truth estimates provided by lab equipment. Our method is the first to propose such a simple capture method for mechanical properties outperforming other methods that require testing the fabric in specific setups.

## CCS Concepts

- Computing methodologies → Computer vision; Neural networks; Computer graphics;

## 1. Introduction

Accurate and trustworthy digital garments, often referred to as *digital twins*, are key for the successful digitalization of the apparel industry. From early prototyping in 3D Computer-Aided Design (CAD) to custom fits in virtual try-on, digital garments have the

potential to transform a centuries-old industry to make it more efficient while reducing its carbon footprint [BHL\*17].

In this context, digital *textiles* are largely responsible for how a garment looks and drapes: they are the building blocks of digital apparel. As such, the optical and mechanical properties of real fab-

rics need to be carefully captured and digitized to faithfully reproduce a garment in the digital world. Yet, in an industry where the transition to digital has become a necessity [HMR<sup>\*</sup>20, RI20], digitizing textiles is a manual process, slow, and expensive [KLBG20]. It requires sophisticated equipment, a skilled workforce, and sometimes even shipping fabric swatches to a lab across the world. These complex pipelines make it difficult for the apparel industry to meet market demands, which often require digitizing hundreds of textile materials within tight time-frames [BHL<sup>\*</sup>17]. The result is a slowdown in the adoption of digital tools by the industry or, even worse, trading accuracy for practicality by choosing from limited preset pools of digital fabrics.

While there are practical solutions for optical digitization [RPDEPHG23, MRR<sup>\*</sup>22], efficient mechanical digitization has been a less explored area of research. Mechanical digitization of fabrics has traditionally required the use of specialized testing devices [KLBG20, Kaw80, Min95] and skilled operators. Therefore, several techniques have attempted to simplify the process by using videos [BJNX18, DBC<sup>\*</sup>15, HEW17] or photographs of the fabric under specific conditions [RPPMCG23, JC20, FHW22] as input data to derive mechanical properties. Despite these efforts, these methods still require specific hardware and laborious manipulations.

To address these limitations and inspired by recent work in the field of optical digitization, which demonstrated that a single image is sufficient to estimate the optical appearance of materials [RPDEPHG23, MRR<sup>\*</sup>22], we propose a method that avoids the use of specialized hardware, requiring only the manufacturer metadata as input. Our key observation is that the fabrication process and the underlying yarn materials have a high influence on the macro-scale mechanical behavior of the fabric [Sü12, HC98, Das13]. As an illustrative example, the straight yarn arrangement in woven fabrics lead to very stiff stretch properties in the warp and weft directions, while the curved yarn loops present in knitted fabrics, allow for more stretching as the yarns become straightened [GO18]. Many other relations have been documented, such as the influence of different woven and knitted families on the stretch and bending properties of the fabric [BM22, AG20, SA<sup>\*</sup>17, CA00] or the effect of different yarn materials on the resulting fabric mechanical properties [Elt16, HC98, SEHEY12, MEA12, KCPN16, Ery19, EGBDC09].

In this work, we introduce two complementary methods that build on this idea. First, we propose a method that regresses the fabric mechanics by taking as input only textile metadata: family, composition, density, and thickness. The *former first two* are typically provided by the manufacturer, while the *latter last two*, if not readily available, can be easily measured using ordinary off-the-shelf tools. We show that using only this information as input we are capable of estimating the mechanical properties of a large and diverse set of fabrics.

Obtaining the fabric family can be challenging for nonspecialists who do not have access to the complete manufacturer technical sheet. Our second method addresses this issue by using planar front and back images of the fabric, instead of the fabric family. We train an end-to-end approach using a neural network to directly regress the mechanical parameters, which yields results comparable to our first solution.

We evaluate both of our methods using quantitative error metrics in the parameter spaces, and an ablation study on the importance and sensibility of each input to the models. However, we also make the observation that using mechanical parameters as error metric struggles to quantify differences in drape, since the particularities of the simulator can make two sets of parameters behave similarly in practice. Therefore, we turn to the Cusick Drape test [ISO08], an industry standard to further understand the accuracy of our method from a perceptual standpoint. To the best of our knowledge, we are the first to provide such an evaluation. In addition, we take a closer look at the resulting models by analyzing them in specific cases to show that they learn nonlinear effects described in the textile literature.

## 2. Related Work

In this section, we discuss methods for estimating mechanical parameters of textiles using testing devices, videos, and photographs. We also survey methods for estimating appearance from single images.

### 2.1. Mechanical Digitization Methods

Evaluating the mechanical properties of real fabrics is a complex task that usually follows a two-step process: acquiring the raw data that captures the mechanical behavior of the fabric, and then using it to derive mechanical parameters *for a specific simulator*. This derivation is, in practice, simulator-specific: in addition to the material model, each simulator makes a number of implementation choices such as the type of discretization and its resolution, or the lenience of convergence thresholds, which can significantly influence the simulation's behavior. The raw data capture is usually done using specialized mechanical testing devices, but there is an increasing research focus on using videos or photographs of the fabric instead.

**Digitization using testing devices.** The use of testing devices is by far the most common approach for textile digitization in the apparel industry [KLBG20]. Most commercial 3D CAD for apparel can derive mechanical parameters from specific devices for their specific simulator. These devices are often manufactured and sold by the same companies developing the 3D CAD software itself.

Some of the most common devices available in the industry are the Kawabata Evaluation System (KES) [Kaw80], the Fabric Assurance by Simple Testing (FAST) [Min95], the Fabric Touch Tester (FTT), the CLO Fabric Kit 2.0 [Clo], the Fabric Analyser by Browzwear (FAB) [Bro] and the Optitex Mark 10 [Opt]. They measure stretch resistance based on uniaxial stretch tests, and bending resistance through cantilever, pearlloop or similar methods [CPGE90]. Once the raw data is generated, usually as sequences of force-deformation datapoints, an estimation method can be used to derive mechanical parameters from it [MTLVL07, SB08, VMTF09, WOR11, MBT<sup>\*</sup>12, CTT17]. The objective is to find the best values for the set of parameters that can accurately explain the raw data when using a specific simulator.

Using a testing device is arguably the best way to obtain the mechanical parameters of a fabric: the specimen itself is tested, exciting the exact deformation modes that need to be characterized.

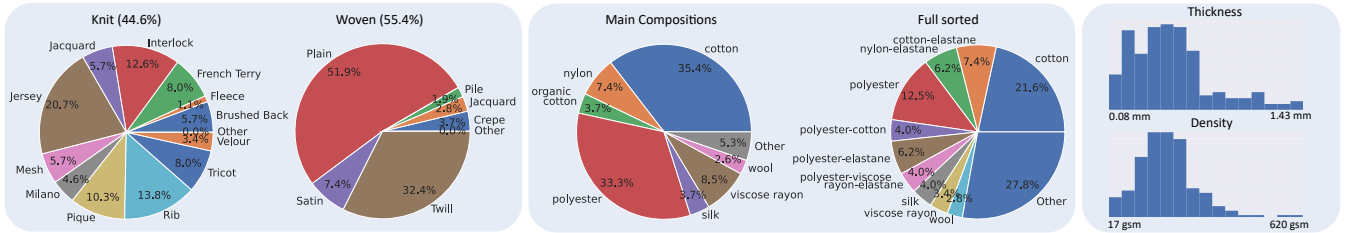


**Figure 2:** Distribution of our dataset. Left, distribution of families for woven and knit structures. Middle, main composition: percentage of fabrics that contain a given composition; full sorted: percentage of fabrics with mixed compositions. Right, histogram of distributions for density and thickness.

However, this approach comes with many drawbacks, mainly from the need to manipulate complex sophisticated machines, making the process slow, manual, expensive, and requiring skilled operators. In addition, it has been observed that two testing devices can produce different results for the same fabric [Pow13], suggesting that even a machine-based approach is not infallible and questioning the very nature of the *ground truth*. To make matters worse, the lack of consensus on standardized simulation models and mechanical tests [KLBG20, Pow13] results in a sort of vendor lock-in. One device is often tied to one CAD, and both raw data and mechanical parameters cannot be interpreted by other CADs, which poses a challenge for interoperability. Recent standardization efforts are trying to address this issue, both by providing some documentation on vendor-specific mechanical parameters [Sub21] and by encouraging the distribution of raw data in an open format [[u3m](#)], but with limited adoption so far.

**Digitization from visual input** It is possible to obtain the mechanical parameters in a less constrained setup, eliminating the need to use specialized hardware and some of the drawbacks that come with it. Video and photographic sources of data can convey abundant mechanical information when the fabric is deformed in the right way. While all methods necessarily rely on doing simulations (we recall that the mechanical parameters are specific to a given simulator), we separate the literature in two categories, each with their own pros and cons: methods that embed simulation steps into the parameter estimation process, and methods that use simulation as a preprocess to build a dataset and learn from it.

In the first category, simulation-optimization methods, simulation is used during parameter estimation in an iterative loop to refine the mechanical parameters until an objective function is satisfied, which is also the method of choice when using data from testing devices [SB08, WOR11, MBT\*12]. Yang *et al.* [YPA\*18] take a single-view image of a garment, and run a joint material-pose estimation of the textiles and the avatar, comparing the location and density of wrinkles and folds of the garment between the photograph and successive simulations to refine the mechanical parameters. Bhat *et al.* [BTH\*03] take a real video sequence of a fabric swatch hanging by its corners under gravity, and uses fold information to optimize a match with simulated video sequences. Similarly, Runia *et al.* [RGSS20] extract wave information from

real and simulated video sequences of flapping flags as metric to optimize the mechanical parameters of the simulation.

In the second category, simulation as preprocess, regression methods are used on simulated datasets to directly learn the deformation space and encode it as a latent feature vector. The mechanical parameters of cloth have been inferred using video data as input [BXBF13, YLL17, BNXJ18], *anwhile* friction can be obtained using photographs that encode reflectance [ZDN16] and videos of the cloth sliding through a surface [RRBD\*20]. Pure data-driven methods such as Huber *et al.* [HEW17] find the most similar cloth in a dataset using a descriptor that encodes motion. Ju *et al.* [JC20] use manually labelled Cusick drape 3D boundaries as input, which Feng *et al.* [FHWX22] later automatized by using multiple-view depth images. Similarly, Rodriguez-Pardo *et al.* [RPPMCG23] use depth images of the fabric hung in a specific configuration and a neural network to analyze them and estimate the mechanical parameters.

Inspired by these methods, and taking it a step further, our approaches only require the metadata of the fabric and, optionally, flat images of the front and back sides of the sample. This removes the need to manually setup and capture the fabric in mechanically expressive configurations, or even having physical access to the fabric itself.

## 2.2. Single Image-based Appearance Estimation

Our approach also draws from current trends in the field of optical material capture. Although several approaches include variable illuminations [AWL\*15] or multiple images as input [DAD\*19], many methods have demonstrated very reasonable accuracy taking as input just a single image with fixed illumination [MRR\*22, HDMR21, LDPT17, LSC18, DAD\*18, WWZ\*22, GLT\*21, VPS21, ZK21]. For the particular case of textiles, recent work [RPDE-PHG23] obtains very low error rates with a single diffuse image taken with a flatbed scanner. This scenario suggest that the semantics of the material –that can be observed in a single image– is a valuable cue to disambiguate its optical appearance properties. We demonstrate that a similar reasoning can be applied for mechanical properties, given that the woven/knitting pattern is key to determine the fabric’s mechanical behavior.

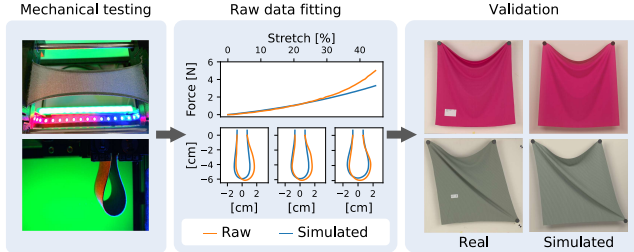


**Figure 3:** Fabric digitization pipeline used to generate the dataset. The fabrics are mechanically tested with proprietary stretch and bending machines, obtaining raw mechanical data. Then, an automatic optimization process finds the simulation model parameters that best fit the data. Lastly, the digitized fabric is validated by comparing it to real photographs.

### 3. Overview

Our goal is to digitize fabrics without requiring to manipulate a fabric sample. To this end, we follow a learning-based regression approach that avoids the need to perform complex simulations or building specific setups by taking the fabric metadata as input.

We gather a dataset of textile materials that we digitize with proprietary lab testing equipment. Section 4 describes the contents of the dataset, the process to build it, and the simulation engine behind it.

Section 5 introduces our two complementary solutions to estimate the mechanical parameters. Our first method, MECHMET, works by using only the manufacturer metadata: density, thickness, percentage of compositions, structure type, and family. Our second method, MECHIM, eliminates the requirement to know the fabric family by using front and back planar images of the fabric sample.

We evaluate our methods using standard error metrics, but also with perceptual metrics used by the textile industry. Section 6 describes these metrics and motivates their importance for this problem. Section 7 presents an exhaustive evaluation of our methods, including an ablation study, several quantitative and qualitative results, and comparisons to the state-of-the-art. Finally, in Section 8 we analyze the learned models to compare their behavior to different observations documented in the textile literature.

### 4. Dataset

We carefully collected a curated set of 1565 real fabrics from a wide variety of families, densities, compositions, and thicknesses. The curation and labeling was done by textile specialists that guaranteed that the set and data was representative of the textile market. Each fabric sample contained information regarding metadata, digital images, and simulation parameters. The dataset has been released [dat] and is freely available for academic use. An extended version of the dataset (including a full texture stack and mechanical parameters for third party vendors) is available at SEDDI Textura [tex].

The metadata was composed of density (gsm)  $\rho \in \mathbb{R}$ , thick-

ness (mm)  $t \in \mathbb{R}$ , percentage of compositions  $c \in \mathbb{R}^{|C|}$  where  $C = \{\text{WOOL, POLYESTER, ANGORA, CASHMERE, RAMIE, MOHAIR, NYLON (POLYAMIDE), RAYON, METALLIC, POLYURETHANE (ELASTANE), BAMBOO, VEGETAL FIBRE, ACETATE, ALPACA, COTTON, SILK, ACRYLIC, HEMP, MODAL, FLAX}\}$ , structure type  $s \in \{\text{WOVEN, KNIT}\}$ , and family  $f$  which is different for knits  $f \in \{\text{INTERLOCK, FRENCH TERRY, FLEECE, BRUSHED BACK FLEECE, VELOUR, TRICOT, RIB, PIQUE, MILANO, MESH, JERSEY, JACQUARD}\}$  and for wovens  $f \in \{\text{PLAIN, PILE, JACQUARD, CREPE, SATIN, TWILL}\}$ . Figure 2 (left) shows the resulting family distribution for knits and wovens. In the middle, we show the distribution of compositions. It is worth noting that our main compositions chart agrees with recent reports of fiber type production and usage [Fer21, Tex21] that state that the majority of fabrics are made of cotton and polyester, followed by rayon and nylon. In the chart *full sorted*, we observe which pairs of compositions are usually tied together, information which is important to understand potential biases in the data. Then, we took front and back planar images of 11x11cm swatches of the fabric using a commodity flatbed scanner at 400 DPIs.

Finally, we mechanically digitized each fabric using proprietary testing equipment and methods. Our digitization process, illustrated in Figure 3, has two steps. In the first step, we capture raw stretch and bending mechanical data in the three main fabric directions (warp, weft and bias), following digital textiles industry practices [KLBG20]. This raw data consists of force-elongation measurements of uniaxial stretch tests, and fabric folding outlines of pearloop bending tests [CPGE90].

In the second step, we run numerical optimizations to obtain the mechanical parameters that, together with the fabric density and thickness taken from the metadata, govern our simulation methods. For this, we use the same mechanical simulator that will be later used to run fabric simulations. Our simulator uses the Finite Element method to discretize the underlying equations of motion over a triangular mesh, and a Newton-Raphson Backward Euler solver to timestep the dynamic simulation. We use the Saint-Venant Kirchoff (StVK) hyperelastic energy to model resistance to stretch [VMTF09] with a quadratic strain and a linear strain/stress relationship, and a discrete hinge energy to model resistance to bending [GHDS03, BMF03]. Both energies are made anisotropic, a natural property of most fabrics, by using different parameters, namely,  $k_{\text{SWarp}}$ ,  $k_{\text{SWeft}}$ ,  $k_{\text{SBias}}$  for stretch and  $k_{\text{BWarp}}$ ,  $k_{\text{BWeft}}$  and  $k_{\text{BBias}}$  for bending in the warp ( $0^\circ$ ), weft ( $90^\circ$ ), and bias ( $45^\circ$ ) directions, respectively. **The bending model is parameterized by a single stiffness value, so we introduce anisotropy by assigning an interpolated stiffness parameter to each hinge based on its orientation in the reference configuration [WOR11].**

We consider this data to be our ground truth, and will use it to train our learning-based models. However, the models we propose are agnostic to the underlying simulator and could be trained on datasets with different mechanical parameterizations. Figure 3 (right) compares photographs of fabric swatches under different drape conditions with their digital replicas. These comparisons were used during the generation of the dataset to qualitatively validate the accuracy of each fabric digitization.

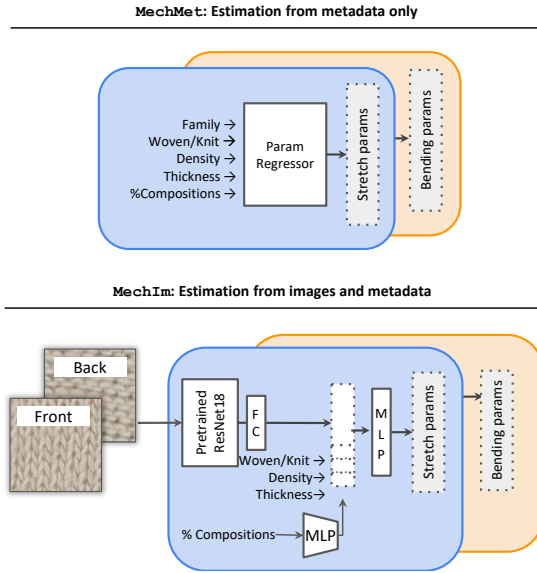


**Figure 4:** Diagram showcasing the two inference models proposed in this work. Notice that MECHMET requires the fabric family as input while MECHIM replace that input with front and back images of the fabric.

## 5. Methods

Estimating a set of real numbers given a variable number of input parameters can be posed as a classic regression problem given a dataset sufficiently large to cover the parameter space. Here we describe our two methods designed to take two different types of inputs, while low level implementation details are described in the Supplementary Material.

### 5.1. MECHMET: Metadata Only as Input

An efficient way to learn a parameter regressor is through the use of Random Forests Regressors (RFR). RFRs are fast to train and evaluate, and can handle both numerical and categorical inputs. Although we experimented with Multi-Layer Perceptrons and achieved similar accuracy, as shown in Section 7, we ultimately chose a Random Forest Regressor for its efficiency. Since the correlation between stretching and bending parameters is not significant [RPPMCG23], we train two independent regressors for stretch and bending parameters. Nevertheless, we also experimented with a single regressor for both sets obtaining less precision in the estimations.

### 5.2. MECHIM: Images and Metadata as Input

Our second solution eliminates the need to have prior knowledge about the fabric family, hard to obtain if not present in the fabric technical sheet and without an expert eye. Instead, this solution takes as input the front and back images of the fabric.

In this setup, a RFR is not sufficiently expressive to take raw images as input. Therefore, we use an end-to-end neural network.

The overview of the architecture is presented in Figure 4 (bottom). First, we stack front and back images as a 6-channel input and extract a feature vector from a pre-trained neural network that serves as feature extractor. This neural network will be fine-tuned during the learning process. The feature vector is then passed through a fully-connected layer (FC) to reduce its dimensionality. While this feature vector is similar to the last layer of a classifier, we have found that explicitly estimating the fabric family gave worse results than implicitly learning fabric features during training (even if our family categorization is reasonable and validated by industry experts, there might be fuzzy categories for which a rigid classification is not advantageous). Afterwards, the resulting feature vector is concatenated with the available metadata (density, structure type, thickness, and compositions) and passed through an MLP that returns the simulation parameters. As before, we train one network for bending and another one for stretch.

In addition, we reduced the dimensionality of the compositions to two dimensions with another MLP learned through the same process. This comes from the empirical observation (Figure 5) that such size reasonably covers the variability of our dataset. Note that we do not perform such reduction in our first model due to the impossibility to learn the parameters of the reduction from the data in an end-to-end fashion.

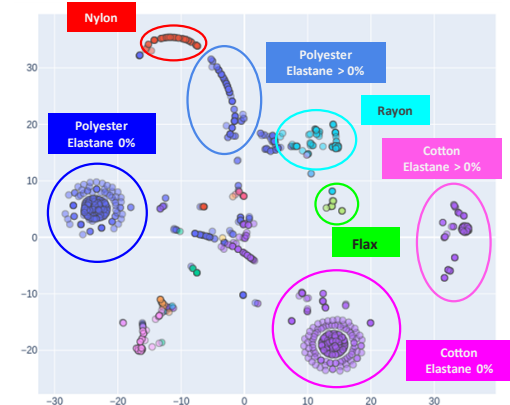


**Figure 5:** Visualization of the dataset after projecting it to two dimensions using tSNE [VdMH08], a dimensionality reduction technique. We observe that samples with and without elastane for the dominant compositions (cotton, polyester) are separated.

## 6. Cusick Drape Metrics

The natural way to quantitatively analyze the accuracy of our models is to measure the error in the parameter space (*i.e.* the six mechanical parameters that describe each fabric). However, as also discussed in previous work [RPPMCG23], these parameters are more related to the internals of the simulator rather than the perceived fabric behavior: they can be misleading when it comes to assessing the accuracy of the fabric *drape*, which is ultimately what matters to the garment designer. Figure 6 illustrates this phenomena. Two fabrics with significantly different mechanical parameters result in very similar drapes: the bending parameters of the fabric

Params	ID-0999	ID-0874
$\rho$	42	149
$kS_{Warp}$	310	278
$kS_{Weft}$	145	278
$kS_{Bias}$	25	179
$kB_{Warp} (10^{-8})$	17	143
$kB_{Weft} (10^{-8})$	17	89
$kB_{Bias} (10^{-8})$	34	68

**Figure 6:** Two fabrics with very different mechanical parameters: 3x in density, up to 7x in stretch, and up to 8x in bending. Yet their Cusick drapes are virtually identical, showing that differences in mechanical parameters don't necessarily reflect differences in drape.

on the right are up to 8 times the ones on the left, yet the draping is virtually identical. There are many factors that can contribute to this phenomenon, including cross effects between stretch and bending, low sensitivity to changes at both ends of the parameter range, and even eventual limitations of the simulator itself.

To address these limitations, we use the Cusick Drape test [Cus65, ISO08], an industry standard for measuring the drape of a fabric. The Cusick test is easy to apply to digital fabrics and provides a set of quantitative values that are easy to interpret in terms of the fabric's qualitative behavior. Additionally, it allows for comparisons between digital fabrics regardless of the underlying simulator.

In the Cusick Test, a circular piece of fabric of 30 cm in diameter drapes under its own weight over a supporting disk of 18 cm in diameter. Using this setup it is possible to compute several metrics. The *Drape Coefficient* (DRPct), expressed in terms of percentage, is the ratio between the area of the outline of the draped fabric and the area of the circular flat piece. The lower the number, the higher the drapability. Many other indicators can be extracted from the Cusick test: Carrera-Gallissà and collaborators [CGCV17] identified 36 different ones in the technical literature. However, after carefully assessing the performance of each indicator, they suggest to focus on the *Drape Coefficient* first, followed by the *Mean Fold Number* (FN) and the *Fold Height* (FH) to discriminate among drapes. The latter are respectively the number of folds of the outline and the average height of those folds (in mm). We therefore augment the analysis of our models with the three aforementioned Cusick Drape metrics.

## 7. Evaluation and Results

In this section, we present a quantitative analysis of the performance of both models using different evaluation metrics. Additionally, we conduct an ablation study of the input parameters. Then, we showcase several results and compare the performance of our method with related work.

### 7.1. Quantitative Evaluation

We use common metrics to numerically evaluate the quality of our models and industry standard metrics to understand drape as described in Section 6. We split our dataset in 1371 fabrics for training and 194 for testing.

First, we use the Normalized Mean Absolute Error (NMAE) and the Spearman correlation metrics to understand the error in the parameter space. To obtain a more comprehensible understanding of the quantitative errors, we normalize the estimations by the minimum and maximum values of the training set. For the computation of the NMAE, we performed a min-max normalization with the maximum and minimum values of the training set, effectively normalizing the data to the [0,1] range, which we then multiplied by 100 to get a percentage. This scaling helps us analyze and interpret the results since mechanical parameters in simulators can have arbitrary ranges (e.g., note the 8 order of magnitude scale difference between stretch and bending values in Figure 6). With this normalization, we transform the errors to more comprehensible values.

The errors shown in Table 1 indicate that the average error in parameter space is below 6% for the average  $kS_{avg}$  of the three stretch parameters and 12% for the average  $kB_{avg}$  of the three bending parameters. Using the fabric family or images as input does not have a significant impact on the estimation of *stretch* parameters, although using the family as input improves the estimation of *bending*. This suggests that our family taxonomy contains semantically meaningful information that may not be immediately visible in the scanned images. It appears that stretch parameters can be more easily identified even if the exact fabric category is known. Interestingly, the stretch bias parameter seems to be the most challenging to estimate given our input. We speculate this is a consequence of the underlying stretch model in our simulator. While  $kS_{Warp}$  and  $kS_{Weft}$  are orthogonal,  $kS_{Bias}$  modulates the shear properties of the fabric [VMTF09]. This effectively makes the stretch in the bias direction depend on the three parameters on the warp and weft parameters as well, forcing regression approaches to infer this more complex relation.

To complement this analysis we also measure the error using the Cusick Test. As previously mentioned (Section 6), these metrics evaluate the drape accuracy in a global and more meaningful way. Tables 1 and 2 report very similar performance between our two models, although MECHMET slightly outperforms MECHIM in all the Cusick metrics. We refer the reader to the supplementary material for a comparison of the virtual Cusick drapes of a varied set of fabrics, showing the ground truth against the results of MECHMET and MECHIM.

### 7.2. Per Family Analysis

We also evaluate the error per family for a more in-depth analysis. The results are shown in Figure 7. We observe that both models perform similarly, particularly for bending parameters. MECHIM struggles with certain classes that are complex to identify in the images such as Twill or Milano which can have very small yarns or be similar to other categories. Plain and Twill groups have the higher variability of errors. This might indicate that splitting them

		Params NMAE $\times 10^0$								Cusick MAE		
		kS <sub>Warp</sub>	kS <sub>Weft</sub>	kS <sub>Bias</sub>	kB <sub>Warp</sub>	kB <sub>Weft</sub>	kB <sub>Bias</sub>	kS <sub>Avg</sub>	kB <sub>Avg</sub>	DRPct	FN	FH
MECHMET	RFR w/o images	<b>6.15</b>	<b>7.52</b>	<b>4.14</b>	<b>11.26</b>	<b>12.35</b>	<b>8.80</b>	<b>5.94</b>	<b>10.80</b>	<b>9.73</b>	<b>0.86</b>	<b>3.02</b>
MECHIM	NN w/o images	6.17	7.71	4.00	11.30	12.90	9.10	5.96	11.10	9.94	0.91	3.33
	FULL	<b>6.31</b>	<b>7.47</b>	<b>4.18</b>	<b>11.81</b>	<b>12.03</b>	<b>9.53</b>	<b>5.99</b>	<b>11.12</b>	<b>10.14</b>	<b>0.89</b>	<b>3.20</b>
	w/o front	7.14	8.76	4.51	12.95	12.55	10.49	6.80	12.00	10.78	0.96	3.31
	w/o back	7.05	8.42	3.92	13.16	13.35	9.92	6.46	12.14	10.55	0.99	3.29
	w/o compositions	6.94	8.47	4.42	12.10	12.52	11.37	6.61	12.00	12.81	1.15	3.71
	w/o thickness	6.20	7.99	4.06	13.25	12.96	10.45	6.08	12.22	11.40	1.07	3.55
	w/o density	6.17	7.75	4.29	12.23	12.54	10.79	6.07	11.85	11.50	0.99	3.56

**Table 1:** Absolute errors of our models with ablation study. Left, error estimates in the mechanical parameter space using NMAE. Right, MAE errors using Cusick metrics.

		Params Spearman							Cusick Spearman			
		kS <sub>Warp</sub>	kS <sub>Weft</sub>	kS <sub>Bias</sub>	kB <sub>Warp</sub>	kB <sub>Weft</sub>	kB <sub>Bias</sub>	kS <sub>Avg</sub>	kB <sub>Avg</sub>	DRPct	FN	FH
MECHMET	RFR w/o images	<b>0.67</b>	<b>0.70</b>	<b>0.56</b>	<b>0.71</b>	<b>0.72</b>	<b>0.76</b>	<b>0.64</b>	<b>0.73</b>	<b>0.70</b>	<b>0.50</b>	<b>0.62</b>
MECHIM	NN w/o images	0.68	0.69	0.59	0.74	0.72	0.76	0.65	0.74	0.74	0.55	0.68
	FULL	<b>0.64</b>	<b>0.71</b>	<b>0.54</b>	<b>0.66</b>	<b>0.66</b>	<b>0.73</b>	<b>0.63</b>	<b>0.68</b>	<b>0.66</b>	<b>0.49</b>	<b>0.57</b>
	w/o front	0.61	0.64	0.36	0.66	0.67	0.70	0.54	0.68	0.62	0.52	0.54
	w/o back	0.63	0.74	0.62	0.60	0.60	0.69	0.66	0.63	0.61	0.40	0.56
	w/o compositions	0.60	0.66	0.34	0.58	0.57	0.66	0.53	0.60	0.48	0.39	0.42
	w/o thickness	0.63	0.66	0.44	0.60	0.58	0.67	0.58	0.62	0.59	0.33	0.53
	w/o density	0.65	0.69	0.46	0.58	0.57	0.63	0.60	0.59	0.57	0.46	0.50

**Table 2:** Correlation coefficients (Spearman) between ground truth and estimated mechanical parameters, as well as between their respective Cusick metrics, for our models and the ablation study.

in more specialized sub-families could help improving the accuracy. Finally, both models struggle with families that are under represented in our dataset, such as Crepe or Fleece.

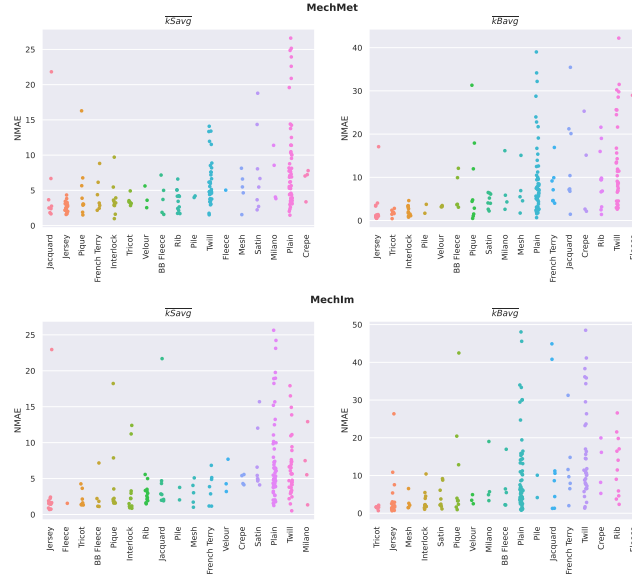


**Figure 7:** (updated figure) Normalized  $\bar{kS}_{avg}$  and  $\bar{kB}_{avg}$  errors of all the fabrics per family, sorted by increasing mean median family error.

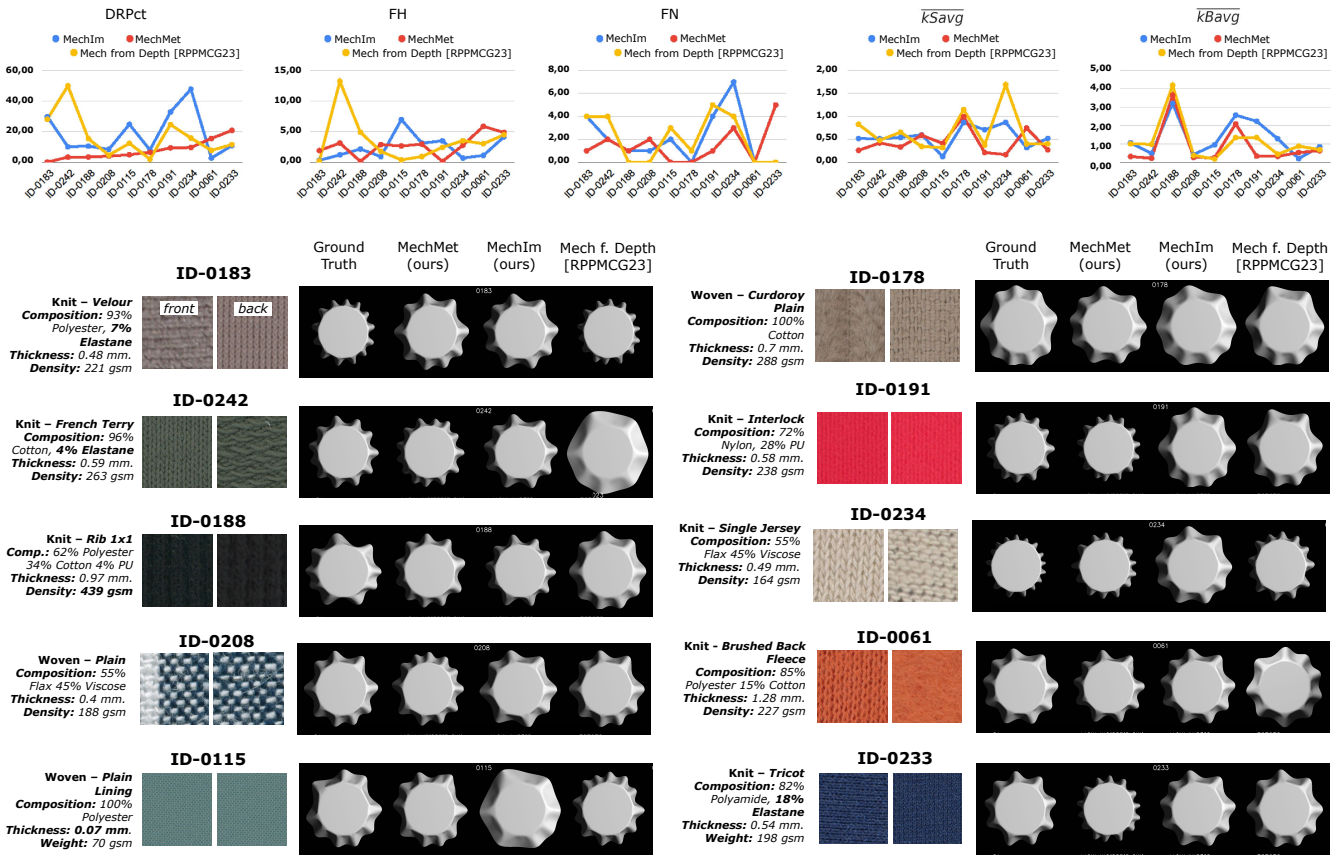
### 7.3. Ablation Study

Table 1 and Table 2 include an ablation study on the input parameters. We study how removing specific inputs impacts the accuracy of the prediction. The study was done using our MECHIM model for convenience but our findings extrapolate to the MECHMET model. Starting from a full model that takes all data as input, we remove components while keeping the same architecture. The results show that removing the input images has the biggest impact in performance. Interestingly, removing the back, which indicates that the back might be more discriminative of the fabric type. However, attending to the Cusick metrics, we observe that the composition is the most important property to take into account, followed by the thickness and the density. As mentioned in Section 6, this illustrates that linear errors in parameter space are not determinant to evaluate the accuracy of the model from a perceptual perspective. Removing density or thickness has similar effect, which aligns with our observation that density and thickness are highly correlated (0.9 in Spearman coefficient).

### 7.4. Qualitative Evaluation and Comparison with Related Work

We compare our models with the method (*Mech from Depth*) of Rodriguez-Pardo *et. al.* [RPPMC23] that uses depth images of the fabric hung in specific setups. We used their train/test split for the comparisons and metrics, which left us with only 10 fabrics for test.

Figure 8 summarizes the results of the comparison. MECHMET model outperforms the other two MECHIM and [RPPMC23] approaches using the drape coefficient metric. This is perceptually visible in the bottom rendersCusick drapes of the figure. The error



**Figure 8: (updated figure)** Comparison with related work. **Top:** absolute errors for Cusick Test and NMAE for mechanical parameters. The fabrics are sorted by increasing error in the drape coefficient (DRPct) of our MECHMET model, which seems to be the best performing one. In light of these results, it appears that the prior information of the fabric family is a strong signal to understand fabric mechanics. **Bottom:** comparison between ground truth (GT) and the different methods (MECHMET, MECHIM, and [RPPMCG23]) for the test set of [RPPMCG23].

in mechanical parameters is very similar among all the models except for fabric ID-0234 that performs very poorly for stretch in the method *Mech from Depth*. Interestingly, this error is not as perceptually visible in the *renders of the Cusick drapes*, nor correlates with the error of the Drape Coefficient (DRPct). This signals the potential bias of the Cusick test towards bending properties, overlooking stretch, aligning with previous observations [FHXW22].

Our model MECHIM particularly struggles with fabrics ID-0191, ID-0234, and ID-0115 for different reasons: ID-0191 has very thin yarns barely visible in the images, ID-0234 **has-a-lot of hairiness in the back images thus confounding the algorithm to recognize that the fabric is single jersey fabric's back has unusually high hairiness for a single jersey fabric, thus confusing the algorithm when trying to recognize its family**, and ID-0115 is a very shiny lining fabric which looks like a satin in the image.

The test set of [RPPMCG23] is very small, making the results particularly sensitive to its contents. For more comprehensive qual-

itative results, we compared our methods with ground truth for our test set of 194 fabrics. This qualitative evaluation can be found in the supplementary material. In addition, in Figure 12 we show different examples of the same dress made with two different fabrics: a stiff denim and a soft interlock. For each fabric, we show the results using ground truth data and both of our methods (MECHMET and MECHIM), with almost indistinguishable drapes.

## 8. Model Inspection

In this section, we identify specific scenarios documented in the scientific textile literature and replicate them by modifying the relevant input parameters in our model. We compare the results in an effort to gain a better understanding of the model's ability to capture the particularities and nonlinear interactions between the fabrication parameters and the resulting mechanical behavior.

Only one relevant input parameter is changed in each case, leaving the rest frozen through the sampling. We acknowledge this is



**Figure 9:** Effect of changing the family of randomly sampled dataset knit fabrics (sorted by density on the horizontal axis) on the output mechanical parameters. The Rib samples tend to decrease resistance to stretch in the weft direction while increase bending resistance in the warp direction w.r.t. the other families, most notably in the denser samples. Pique samples, on the other hand, show slightly higher stretch resistance w.r.t. their Jersey counterparts.

not an ideal setup since the input parameters are not always orthogonal (e.g., changing the family of a knitted fabric using the same yarn is likely to change its thickness too), but given the impossibility to obtain all the ground truth metadata for all the evaluated input samples, we resort to this simpler, more controllable approach and validate if the documented trends are observable. We focus the analysis on the MECHMET model for the same reason. A similar study could be devised for MECHIM, but it would require a careful treatment to avoid conflicting matches between the input images and the rest of the metadata.

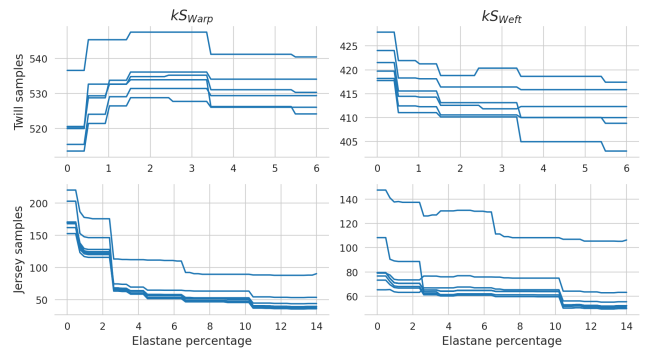
**Elastane on Stretch.** One well documented case is the effect of elastane in different fabric families. When applied to denim (i.e., twill) fabrics, it is typically introduced in the weft yarns, making the fabric stretchier in that direction [KCPN16, Ery19, EGBDC09]. When applied to jersey knits, the effect is notable in the warp direction and, since the weft stretch is dominated by the straightening of the knitted yarns, the effect of elastane in weft stretch can be less significant [Elt16].

We replicate these cases by selecting several twill and jersey fabrics from our dataset with 100% cotton or polyester composition and sweep the composition to reach 6% and 14% elastane for the twill and jersey samples, respectively. Figure 10 shows the output of the model for the stretch parameters, showing that these nonlinear, family-dependent effects, are implicitly captured. Note that the model captures the direction-dependent effects even though our composition input does not discriminate among warp and weft compositions of woven fabrics.

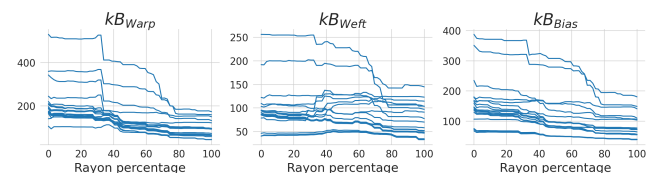
**Rayon on Bending.** Another well documented effect is that of rayon on bending. In particular, woven fabrics with rayon have significantly lower bending rigidity than equivalent fabrics with cotton [HC98, Cus65]. Again, we select a few woven fabrics of different families with 100% cotton composition and sweep the composition to reach 100% rayon.

Figure 11 shows the bending parameters output by the model for the sampled fabrics, showing the notable decrease in the bending parameters as the rayon increases.

**Knit Families.** The effects of fabric family and mechanical properties has also been extensively investigated and documented. One



**Figure 10:** Effect of changing elastane percentage of randomly sampled dataset jersey and twill fabrics on the output mechanical parameters. As elastane increases in jersey fabrics, the resistance to stretch is decreased in warp and weft directions, but more notably in the warp direction. A different effect is observed in the case of twill fabrics, for which the stretch resistance decreases only in the weft direction.



**Figure 11:** Effect of changing rayon percentage of randomly sampled dataset woven fabrics on the output mechanical parameters. As rayon increases, a clear trend appears, reducing bending resistance in all directions, most notably in originally stiffer fabrics.

significant difference is found between jerseys and ribs, the latter being easier to stretch in the weft direction due to the rest configuration induced by the particular stitching pattern [SA\*17]. The same structural properties lead to an increase of the bending resistance of rib fabrics in the warp direction [AMNT00]. Pique knits, on the other hand, show slightly stiffer stretch properties w.r.t. jersey knits due to the presence of tuck loops [AG20].

Figure 9 shows the mechanical properties output by the model for randomly sampled knitted fabrics from the database (sorted by density) when changing their family, showing good agreement with the aforementioned effects.

## 9. Conclusions

We have presented two learning-based methods to estimate the mechanical parameters of fabrics without requiring specific testing devices. The first method requires just the metadata of the fabric as input. The second method removes the need to provide the fabric family by using planar front and back images of the fabric.

We extensively evaluated both models quantitatively and qualitatively, leveraging both common metrics and metrics derived from the Cusick Test, an industry standard that quantifies fabric drape. Our analysis shows good performance, yielding similar or improved results compared to a state-of-the-art method that relies on depth images. In addition, we have validated that our approach can reproduce complex nonlinear effects of the textile fabrication process documented in the scientific literature. These findings support our initial hypothesis that the fabric metadata contains key information regarding its macro-scale mechanical behavior.

However, our approach is not free of limitations. We would like to explore more deeply our family categories to account for a higher variety of fabrication processes (e.g. adding a higher granularity for plain or twill categories). In this sense, we would like to include in our model other fabrication parameters that are known to contribute to this variability, such as yarn tension during weaving [Sü12], or applied finishing [EKBSK19, Ery19].

Improving our visual model is another potential area of research so that we are more robust to variable image quality and able to implicitly account for some of the effects previously mentioned.

Finally, given the limitations in the sensitivity to stretch of the Cusick Test, we would like to continue exploring better ways to evaluate these properties.

**Acknowledgments** The authors would like to thank Dr. Rosa Sánchez-Banderas for helping with the implementation of the Cusick scenes and metrics. This work was funded in part by the Spanish Ministry of Science, Innovation and Universities (MCIN/AEI/10.13039/501100011033) and the European Union NextGenerationEU/PRTR programs through the TaiLOR project (CPP2021-008842). Dr. Elena Garces was partially supported by a Juan de la Cierva - Incorporacion Fellowship (IJC2020-044192-I).

## References

- [AG20] ASSEFA A., GOVINDAN N.: Physical properties of single jersey derivative knitted cotton fabric with tuck and miss stitches. *Journal of Engineered Fibers and Fabrics* 15 (2020), 2, 10
- [AMNT00] ALIMAA D., MATSUO T., NAKAJIMA M., TAKAHASHI M.: Effects of yarn bending and fabric structure on the bending properties of plain and rib knitted fabrics. *Textile Research Journal* 70, 9 (2000), 783–794. 10
- [AWL\*15] AITTALA M., WEYRICH T., LEHTINEN J., ET AL.: Two-shot svbrdf capture for stationary materials. *ACM Transactions on Graphics (ToG)* 34, 4 (2015), 110–1. 3
- [BHL\*17] BERG A., HEDRICH S., LANGE T., MAGNUS K.-H., MATH-EWS B.: The apparel sourcing caravan's next stop: Digitization, 2017. 1, 2
- [BJNX18] BI W., JIN P., NIENBORG H., XIAO B.: Estimating mechanical properties of cloth from videos using dense motion trajectories: Human psychophysics and machine learning. *Journal of vision* 18, 5 (2018), 12–12. 2, 3
- [BM22] BEGUM M. S., MILAŠIŪ R.: Factors of weave estimation and the effect of weave structure on fabric properties: A review. *Fibers* 10, 9 (2022), 74. 2
- [BMF03] BRIDSON R., MARINO S., FEDKIW R.: Simulation of clothing with folds and wrinkles. *ACM SIGGRAPH/Eurographics Symposium on Computer Animation* (01 2003). doi:10.1145/1198555.1198573. 4
- [Bro] Browzwear Fabric Analyzer. <https://browzwear.com/products/fabric-analyzer>. Accessed: 2023-03-05. 2
- [BTH\*03] BHAT K. S., TWIGG C. D., HODGINS J. K., KHOSLA P. K., POPOVIC Z., SEITZ S. M.: Estimating Cloth Simulation Parameters from Video. In *Symposium on Computer Animation* (2003), The Eurographics Association. 3
- [BXBF13] BOUMAN K. L., XIAO B., BATTAGLIA P., FREEMAN W. T.: Estimating the material properties of fabric from video. In *Proc. IEEE International Conference on Computer Vision* (2013), pp. 1984–1991. 3
- [CA00] CHOI M.-S., ASHDOWN S. P.: Effect of changes in knit structure and density on the mechanical and hand properties of weft-knitted fabrics for outerwear. *Textile Research Journal* 70, 12 (2000), 1033–1045. 2
- [CGCV17] CARRERA-GALLISSÀ E., CAPDEVILA X., VALLDEPERAS J.: Evaluating drape shape in woven fabrics. *The Journal of The Textile Institut* 108, 3 (2017), 325–336. doi:10.1080/00405000.2016.1166804. 6
- [Clo] Clo fabric kit 2.0. [https://www.youtube.com/watch?v=HA7HoK6\\_4Fk](https://www.youtube.com/watch?v=HA7HoK6_4Fk). Accessed: 2022-07-07. 2
- [CPGE90] CLAPP T. G., PENG H., GHOSH T. K., EISCHEN J. W.: Indirect measurement of the moment-curvature relationship for fabrics. *Textile Research Journal* 60, 9 (1990), 525–533. 2, 4
- [CTT17] CLYDE D., TERAN J., TAMSTORF R.: Modeling and data-driven parameter estimation for woven fabrics. In *Proceedings of the ACM SIGGRAPH/Eurographics Symposium on Computer Animation* (2017), pp. 1–11. 2
- [Cus65] CUSICK G. E.: The dependence of fabric drape on bending and shear stiffness. *Journal of the Textile Institute* 56, 11 (1965), T596–T606. 6, 9
- [DAD\*18] DESCHAINTRE V., AITTALA M., DURAND F., DRETTAKIS G., BOUSSEAU A.: Single-image svbrdf capture with a rendering-aware deep network. *ACM Transactions on Graphics (ToG)* 37, 4 (2018), 1–15. 3
- [DAD\*19] DESCHAINTRE V., AITTALA M., DURAND F., DRETTAKIS G., BOUSSEAU A.: Flexible svbrdf capture with a multi-image deep network. In *Computer graphics forum* (2019), vol. 38, Wiley Online Library, pp. 1–13. 3
- [Das13] DAS A.: Testing and statistical quality control in textile manufacturing. In *Process control in textile manufacturing*. Elsevier, 2013, pp. 41–78. 2
- [dat] Fabric dataset. <https://drive.google.com/file/d/1h9s10KAjyRF2lF-4QSes5D8TjeoS9G6j/view?usp=sharing>. Accessed: 2024-02-02. 4



**Figure 12:** A dress made with two different materials: a black denim (265gsm, 75% cotton, 25% polyester), and a red interlock (146gsm, 100% modal). Both materials were digitized using capture equipment (Ground Truth) and both of our methods (MECHMET and MECHIM). The images show how the black and red materials are significantly different from each other, while the three versions (Ground Truth, MECHMET and MECHIM) of each material are almost identical.

- [DBC\*15] DAVIS A., BOUMAN K. L., CHEN J. G., RUBINSTEIN M., DURAND F., FREEMAN W. T.: Visual vibrometry: Estimating material properties from small motion in video. In *Proceedings of the ieee conference on computer vision and pattern recognition* (2015), pp. 5335–5343. 2
- [EGBDC09] EL-GHEZAL S., BABAY A., DHOUIB S., CHEIKHROUHOU M.: Study of the impact of elastane's ratio and finishing process on the mechanical properties of stretch denim. *The Journal of The Textile Institute* 100, 3 (2009), 245–253. 2, 9
- [EKBSK19] ERYURUK S. H., KURSUN BAHADIR S., SARICAM C., KALAOGLU F.: The effects of finishing processes on the dynamic drape of wool fabrics. *International Journal of Clothing Science and Technology* 31, 2 (2019), 195–206. 10
- [Elt16] ELTAHAN E.: Effect of lycra percentages and loop length on the physical and mechanical properties of single jersey knitted fabrics. *Journal of Composites* 2016 (2016). 2, 9
- [Ery19] ERYURUK S. H.: The effects of elastane and finishing processes on the performance properties of denim fabrics. *International Journal of Clothing Science and Technology* 31, 2 (2019), 243–258. 2, 9, 10
- [Fer21] FERNANDEZ L.: Distribution of textile fibers production worldwide in 2020, by type, 2021. URL: <https://www.statista.com/statistics/1250812/global-fiber-production-share-type/>. 4
- [FHWXW22] FENG X., HUANG W., XU W., WANG H.: Learning-based bending stiffness parameter estimation by a drape tester. *ACM Transactions on Graphics (TOG)* 41, 6 (2022), 1–16. 2, 3, 8
- [GHDS03] GRINSPUN E., HIRANI A. N., DESBRUN M., SCHRÖDER P.: Discrete shells. In *Proceedings of the 2003 ACM SIGGRAPH/Eurographics symposium on Computer animation* (2003), Citeseer, pp. 62–67. 4
- [GLT\*21] GUO J., LAI S., TAO C., CAI Y., WANG L., GUO Y., YAN L.-Q.: Highlight-aware two-stream network for single-image svbrdf acquisition. *ACM Transactions on Graphics (TOG)* 40, 4 (2021), 1–14. 3
- [GO18] GONG H., OZGEN B.: Fabric structures: Woven, knitted, or nonwoven. In *Engineering of high-performance textiles*. Elsevier, 2018, pp. 107–131. 2
- [HC98] HU J., CHAN Y.-F.: Effect of fabric mechanical properties on drape. *Textile Research Journal* 68, 1 (1998), 57–64. 2, 9
- [HDMR21] HENZLER P., DESCHAINTRE V., MITRA N. J., RITSCHEL T.: Generative modelling of brdf textures from flash images. *ACM Transactions on Graphics (Proc. SIGGRAPH Asia)* 40, 6 (2021). 3
- [HEW17] HUBER M., EBERHARDT B., WEISKOPF D.: Cloth animation retrieval using a motion-shape signature. *IEEE Computer Graphics and Applications* 37, 6 (2017), 52–64. 2, 3
- [HMR\*20] HÄMMERLE V., MÜHLENBEIN C., RÜSSMANN M., GAUGER C., ROHRHOFER S.: Why fashion must go digital—end to end, 2020. 2
- [ISO08] *Textiles — Test methods for nonwovens — Part 9: Determination of drapability including drape coefficient*. Standard, International Organization for Standardization, Geneva, CH, 2008. 2, 6
- [JC20] JU E., CHOI M. G.: Estimating cloth simulation parameters from a static drape using neural networks. *IEEE Access* 8 (2020), 195113–195121. 2, 3
- [Kaw80] KAWABATA S.: The standardization and analysis of hand evaluation. *The Textile Machinery Society of Japan* (1980). 2
- [KCPN16] KUMAR S., CHATTERJEE K., PADHYE R., NAYAK R.: Designing and development of denim fabrics: Part 1-study the effect of fabric parameters on the fabric characteristics for women's wear. *Journal of Textile Science & Engineering* 6, 4 (2016). 2, 9
- [KLBCG20] KUIJPERS S., LUIBLE-BÄR C., GONG R. H.: The measurement of fabric properties for virtual simulation—a critical review. *IEEE SA INDUSTRY CONNECTIONS* (2020), 1–43. 2, 3, 4
- [LDPT17] LI X., DONG Y., PEERS P., TONG X.: Modeling surface appearance from a single photograph using self-augmented convolutional neural networks. *ACM Transactions on Graphics (ToG)* 36, 4 (2017), 1–11. 3
- [LSC18] LI Z., SUNKAVALLI K., CHANDRAKER M.: Materials for masses: Svbrdf acquisition with a single mobile phone image. In *Proceedings of the European Conference on Computer Vision (ECCV)* (2018), pp. 72–87. 3
- [MBT\*12] MIGUEL E., BRADLEY D., THOMASZEWSKI B., BICKEL B., MATUSIK W., OTADUY M. A., MARSCHNER S.: Data-driven estimation of cloth simulation models. In *Computer Graphics Forum* (2012), vol. 31, Wiley Online Library, pp. 519–528. 2, 3
- [MEA12] MOURAD M., ELSHAKANKERY M., ALMETWALLY A. A.:

- Physical and stretch properties of woven cotton fabrics containing different rates of spandex. *Journal of American Science* 8, 4 (2012), 567–572. 2
- [Min95] MINAZIO P. G.: Fast-fabric assurance by simple testing. *International Journal of Clothing Science and Technology* (1995). 2
- [MRR\*22] MARTIN R., ROULLIER A., ROUFFET R., KAISER A., BOUBEKEUR T.: Materia: Single image high-resolution material capture in the wild. *Computer Graphics Forum (Proc. EUROGRAPHICS 2022) to appear*, to appear (2022), to appear. 2, 3
- [MTLVL07] MAGNENAT-THALMANN N., LUIBLE C., VOLINO P., LYARD E.: From measured fabric to the simulation of cloth. In *2007 10th IEEE International Conference on Computer-Aided Design and Computer Graphics* (2007), IEEE, pp. 7–18. 2
- [Opt] Optitex Mark-10. <https://optitex.com/products/fabric-management/>. Accessed: 2023-03-05. 2
- [Pow13] POWER J.: Fabric objective measurements for commercial 3d virtual garment simulation. *International Journal of Clothing Science and Technology* (2013). 3
- [RGSS20] RUNIA T. F., GAVRILYUK K., SNOEK C. G., SMEULDERS A. W.: Cloth in the wind: A case study of physical measurement through simulation. In *Proceedings of the IEEE/CVF Conference on Computer Vision and Pattern Recognition* (2020), pp. 10498–10507. 3
- [RI20] ROBERTS-ISLAM B.: Is digitization the savior of the fashion industry?, 2020. 2
- [RPDEPHG23] RODRIGUEZ-PARDO C., DOMINGUEZ-ELVIRA H., PASCUAL-HERNANDEZ D., GARCES E.: UMat: Uncertainty-Aware Single Image High Resolution Material Capture. *Proc. of Computer Vision and Pattern Recognition (CVPR 2023)* (2023). 2, 3
- [RPPMCG23] RODRIGUEZ-PARDO C., PRIETO-MARTIN M., CASAS D., GARCES E.: How Will It Drape Like? Capturing Fabric Mechanics from Depth Images. *Computer Graphics Forum (Proc. Eurographics) 2*, 42 (2023). 2, 3, 5, 7, 8
- [RRBD\*20] RASHEED A. H., ROMERO V., BERTAILS-DESCOUBES F., WUHRER S., FRANCO J.-S., LAZARUS A.: Learning to measure the static friction coefficient in cloth contact. In *Proceedings of the IEEE/CVF Conference on Computer Vision and Pattern Recognition* (2020), pp. 9912–9921. 3
- [SA\*17] SITOTAW D. B., ADAMU B. F., ET AL.: Tensile properties of single jersey and 1×1 rib knitted fabrics made from 100% cotton and cotton/lycra yarns. *Journal of Engineering* 2017 (2017). 2, 10
- [SB08] SYLLEBRANQUE C., BOIVIN S.: Estimation of mechanical parameters of deformable solids from videos. *The Visual Computer* 24, 11 (2008), 963–972. 2, 3
- [SEHEY12] SADEK R., EL-HOSSINI A., ELDEEB A., YASSEN A.: Effect of lycra extension percent on single jersey knitted fabric properties. *Journal of Engineered Fibers and Fabrics* 7, 2 (2012), 155892501200700203. 2
- [Sub21] SUBCOMMITTEE D. I.: Standard operating procedures for digital fabric physics interoperability, 2021. 3
- [Stü12] SÜLE G.: Investigation of bending and drape properties of woven fabrics and the effects of fabric constructional parameters and warp tension on these properties. *Textile Research Journal* 82, 8 (2012), 810–819. 2, 10
- [tex] SEDDI Textura. <https://textura.ai/>. Accessed: 2024-02-02. 4
- [Tex21] TEXTILE EXCHANGE: Preferred fiber & materials market report 2021. *Textile Exchange: Lamesa, TX, USA* (2021). 4
- [u3m] Unified 3D Material (U3M). <https://browzwear.com/about-u3m>. Accessed: 2023-03-05. 3
- [VdMH08] VAN DER MAATEN L., HINTON G.: Visualizing data using t-sne. *Journal of machine learning research* 9, 11 (2008). 5
- [VMTF09] VOLINO P., MAGNENAT-THALMANN N., FAURE F.: A simple approach to nonlinear tensile stiffness for accurate cloth simulation. *ACM Transactions on Graphics* 28, 4 (2009), Article–No. 2, 4, 6
- [VPS21] VECCHIO G., PALAZZO S., SPAMPINATO C.: Surfacenet: Adversarial svbrdf estimation from a single image. In *Proceedings of the IEEE/CVF International Conference on Computer Vision (ICCV)* (2021), pp. 12840–12848. 3
- [WOR11] WANG H., O'BRIEN J. F., RAMAMOORTHI R.: Data-driven elastic models for cloth: modeling and measurement. *ACM transactions on graphics (TOG)* 30, 4 (2011), 1–12. 2, 3, 4
- [WWZ\*22] WEN T., WANG B., ZHANG L., GUO J., HOLZSCHUCH N.: Svbrdf recovery from a single image with highlights using a pre-trained generative adversarial network. In *Computer Graphics Forum* (2022), Wiley Online Library. 3
- [YLL17] YANG S., LIANG J., LIN M. C.: Learning-based cloth material recovery from video. In *Proceedings of the IEEE International Conference on Computer Vision* (2017), pp. 4383–4393. 3
- [YPA\*18] YANG S., PAN Z., AMERT T., WANG K., YU L., BERG T., LIN M. C.: Physics-inspired garment recovery from a single-view image. *ACM Transactions on Graphics (TOG)* 37, 5 (2018), 1–14. 3
- [ZDN16] ZHANG H., DANA K., NISHINO K.: Friction from reflectance: Deep reflectance codes for predicting physical surface properties from one-shot in-field reflectance. In *European Conference on Computer Vision* (2016), Springer, pp. 808–824. 3
- [ZK21] ZHOU X., KALANTARI N. K.: Adversarial single-image svbrdf estimation with hybrid training. In *Computer Graphics Forum* (2021), vol. 40, Wiley Online Library, pp. 315–325. 3